GRADUATE AERONAUTICAL LABORATORIES
CALIFORNIA INSTITUTE OF TECHNOLOGY

FINAL REPORT

NASA Grant No. NSG-7508

NONLINEAR INTERACTIONS IN SUPERFLUID DYNAMICS: NONSTATIONARY HEAT TRANSFER DUE TO SECOND SOUND SHOCK WAVES

H. W. Liepmann
J. R. Torczynski

Firestone Flight Sciences Laboratory

Guggenheim Aeronautical Laboratory

Karman Laboratory of Fluid Mechanics and Jet Propulsion

Pasadena

FINAL REPORT

Grant No. NSG-7508

National Aeronautics and Space Administration

NONLINEAR INTERACTIONS IN SUPERFLUID DYNAMICS: NONSTATIONARY HEAT TRANSFER DUE TO SECOND SOUND SHOCK WAVES

H. W. Liepmann

J. R. Torczynski

Graduate Aeronautical Laboratories

California Institute of Technology

Pasadena, California

31 January 1983

Introduction

The breakdown of superfluidity remains one of the most interesting aspects of the physics of Helium II. Of principal concern is the occurrence of additional dissipation during counterflow experiments with large heat fluxes. When the relative velocity between normal and super components exceeds a certain value, the two components can no longer be thought of as noninteracting fluids. Rather, new dissipative mechanisms come into play and limit the maximum counterflow velocity obtained.

This "critical" dissipation can be characterized by a fundamental, or intrinsic, critical velocity[1]. By fundamental or intrinsic, it is meant that this critical velocity is geometry independent (and frame invariant). Previous investigators had studied critical velocities, but their experiments were performed in constricted geometries, such as closely packed powders[2], porous materials[3,4] and thin films of helium on glass cylinders[5]. However, since it is intrinsic, this critical velocity should be able to be observed out in the bulk fluid (away from walls).

A second sound shock wave is the ideal method for setting up counterflows and studying the intrinsic critical velocity in bulk fluid. Planar second sound shocks provide an abrupt change of flow state, impulsively accelerating quiescent fluid to a finite uniform relative velocity. This change is accomplished in less than a microsecond, the length of time required for a shock to travel its own thickness. Furthermore, wall effects can be eliminated by time resolution because they require a finite amount of time to propagate inward from the walls. Moreover, the wave fronts remain extremely planar even with the strongest shocks, as schlieren photography has revealed, so the motion remains one-dimensional.

To date our experimental work with second sound shock waves falls into two major categories. The first involves using second sound shocks to measure the temperature and pressure dependence of the intrinsic critical velocity. The results are then compared with the work of Notarys[9]. The second effort entails studying the role of vorticity in the breakdown of superfluidity. It has long been hypothesized[6] that the breakdown of superfluidity involves the production of vorticity, particularly quantized line and ring vortices in the super component, and this has been investigated using a rotating second sound shock tube and a rotating second sound scattering cavity.

Equipment

Essential to all of our experimental work has been the production and detection of second sound shock waves. In our studies we have constructed second sound shock tubes of the following general type (see Fig. 1). The heat pulse is produced by driving a rectangular pulse of current through a thin film Joule heater. This heater, a 1000 Å thick Nichrome film which has been vacuum deposited upon an optically flat quartz substrate, is tightly sealed to one end of a tube of uniform rectangular or circular cross section.

At the other end of the tube, a thin film superconducting sensor records the arrival of the shock wave. A typical sensor consists of a layer of tin deposited atop a layer of gold. This double layer is scribed to produce a long narrow current path and thus a high value of the normal resistance. In order to use one sensor throughout the available temperature range, the sensor layer thicknesses are chosen so that the sensor has a transition temperature of about 2.2 K. An electromagnet installed behind the sensor permits one to decrease the

SECOND SOUND SHOCK TUBE

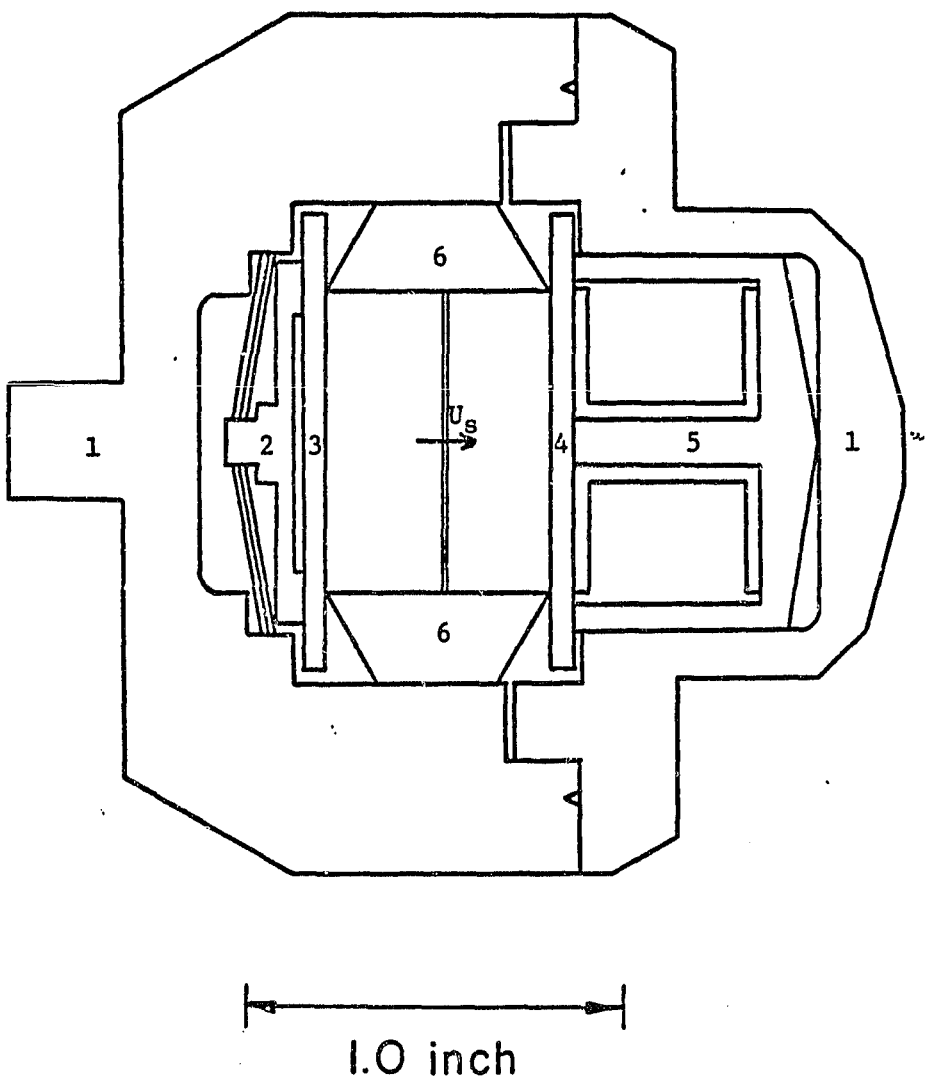

Figure 1. Second sound shock tube. Labeled parts are the following:

1. Brass housing.
2. Spring loading for heater.
3. Quartz substrate of heater.
4. Quartz substrate of sensor.
5. Sensor biasing magnet (superconducting).
6. Teflon tube, down which the shock propagates.

transition temperature by increasing the magnetic field. With the sensors magnetically biased so that the midpoint of the superconducting transition corresponds to the experimental temperature, a constant current, typically about 1 mA, is passed through the sensor. When a second sound wave is incident upon the sensor, its temperature perturbation produces a resistance perturbation and hence a voltage perturbation across the sensor. To calibrate the sensor, a response curve of voltage vs. temperature is obtained by slowly varying the saturated vapor pressure, and hence the temperature of the surrounding liquid helium bath (see Fig. 2). In the course of an actual experiment, both the arrival time (t_A) and the temperature jump (ΔT) are measured with the sensor. The Mach number of the shock wave is given by $M = \frac{L}{at_A}$, where L is the shock tube length and a is the second sound velocity.

In the course of our varied investigations, several second sound shock tubes have been designed and built. One of these is the variable length shock tube, which has a movable endwall sensor that may be located from 2 to 20 cm from the heater. In this manner the time evolution of a second sound shock may be observed by firing several identical strength shocks with the sensor located at different positions along the shock tube. Another shock tube is the optical shock tube, so named because two of its sides are parallel, optically flat quartz windows. This shock tube (in conjunction with our optical dewar) has been used to observe second sound phenomena with optical techniques. Our newest shock tube, the rotating shock tube, combines features of the previously mentioned shock tubes. The sensors are magnetically biased as in the variable length shock tube, and the shock tube is pressurizable to several atmospheres, as is the optical shock tube. However, the rotating shock tube is modular, allowing rapid conversion from one type of cross section to another. For example, the present cylindrical tube could be replaced by one of square cross section

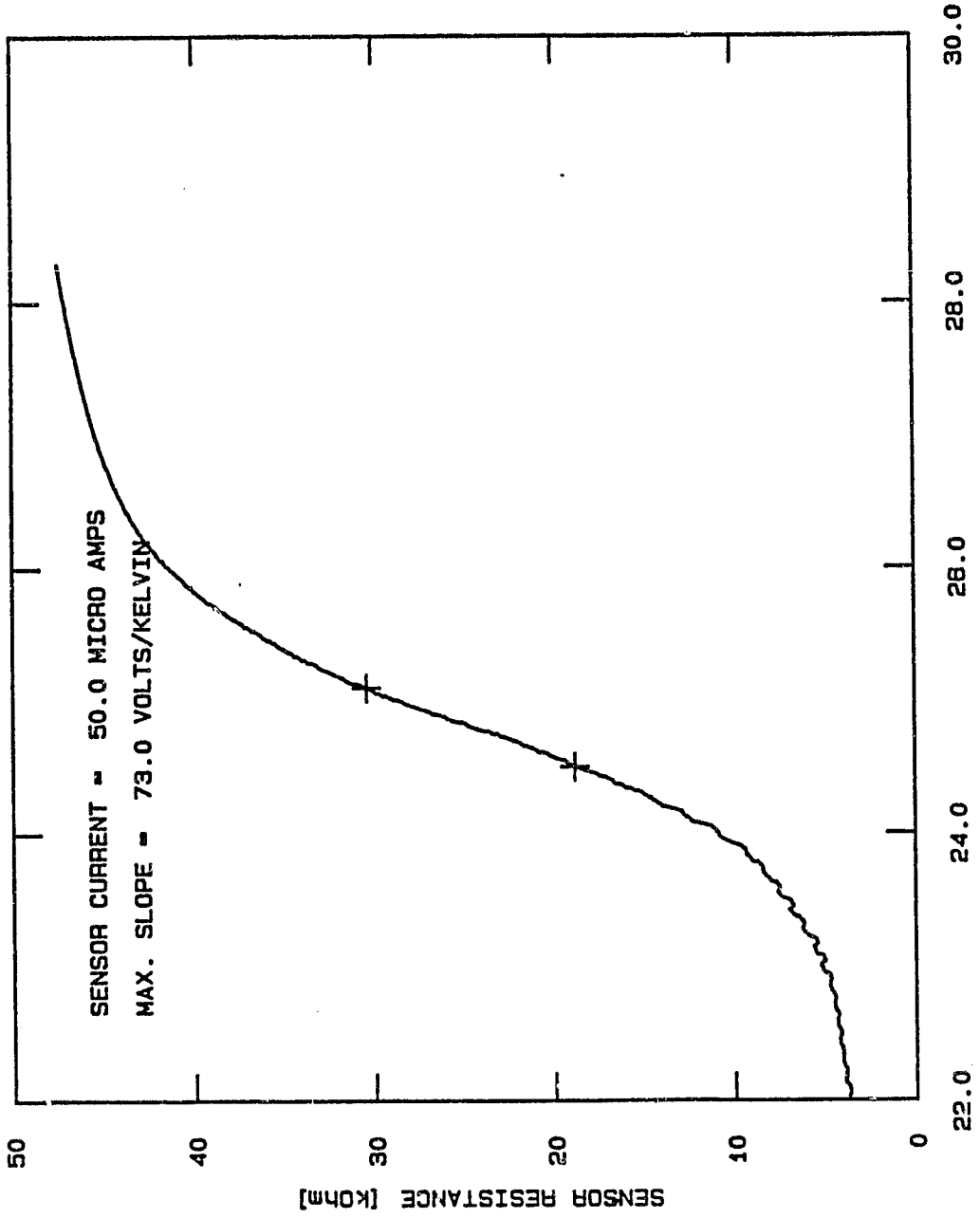

Figure 2. Calibration curve of a granular aluminum superconducting sensor.

without changing the rest of the shock tube. The rotating shock tube is of sufficiently small size so that it may be mounted in one of two orientations in our rotating dewar. In this way, shocks may be fired so as to propagate parallel to the axis of rotation (axial mode) or perpendicular to it (transverse mode).

As mentioned above, it was necessary to design and assemble a rotating liquid helium system. We were fortunate to have available to us a Genisco rotating table capable of rotation rates from 0.01 to 2000°/sec (a more practical limit with a full load is about 540°/sec) with a stability of 0.01%. Atop the 24" diameter stainless steel rotating tabletop is mounted an aluminum frame supporting a standard glass dewar arrangement (see Fig. 3). Two twin vacuum lines emerge from the top of the dewar and are connected underneath the tabletop to the axial vacuum line which passes through a rotating vacuum coupling into the main lab vacuum system. Electrical contact to the rotating system is made through 24 slip rings. The rotating system has about five hours of useful run time per helium fill.

Critical Velocity Experiments

One of our major efforts over the past several years has been to study the fundamental critical velocity in superfluid helium. This critical velocity differs from "extrinsic" critical velocities in that the dissipation arises from a normal component/super component interaction, whereas the extrinsic critical velocities arise from fluid/wall interactions. Thus, it should be possible to observe and study this critical interaction in the bulk fluid, away from walls, so that the fundamental interaction is not influenced by other dissipative effects. By doing many such experiments at different temperatures and pressures, the measured fundamental critical velocity may be compared with theoretical results.

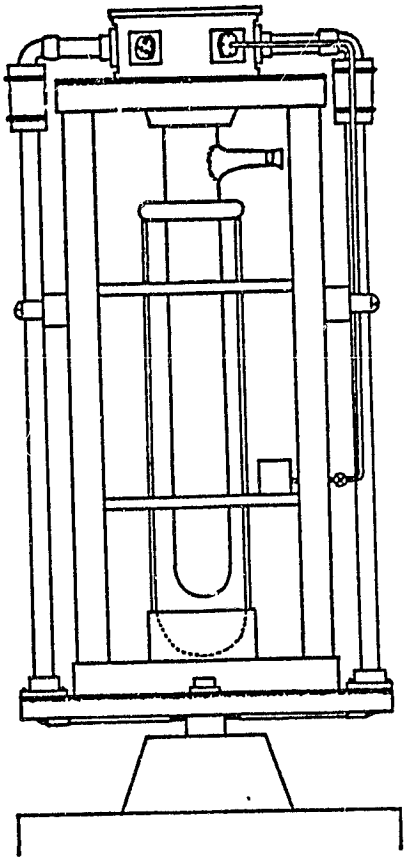

Figure 3. Rotating Dewar

A typical experiment is described below. First, a point $(T_o p_o)$ in the pressure-temperature plane is selected (see Fig. 4) for the experiment. Next, a series of rectangular voltage pulses of increasing strength are fired across the heater. A several minute wait is allowed between the pulses so that the fluid may return to equilibrium. For each pulse the arrival time (corresponding to the average Mach number) and the temperature jump are measured (see Fig. 5 for a typical shock profile). The Mach number is computed and compared with the theoretical results

$$M = 1 + \frac{1}{2}B(p_o,T_o)\frac{\Delta T}{T}$$

$$B(p,T) = T\left[\frac{\partial}{\partial T}\right]_p \ln\left[\frac{a^3 c_p}{T}\right]$$

which have been derived assuming that w/a, the ratio of the relative velocity to the second sound velocity, is small[7].

Shown in Figure 6 are the results of one such experiment ($p_o = 6.0$ *Torr*, $T_o = 1.609$ *K*), scaled so that the second order result (for $\frac{w}{a} << 1$) falls on 45° line. Note that the data follow the theoretical curve quite well until $M = 1.03$. The data dramatically depart from predicted values for higher heater powers; in fact, the average Mach number actually decreases as heater power is increased, showing that there is a limit to the temperature jump (and hence the relative velocity) produced by a second sound shock wave. Curves such as these are typical for all temperatures and pressures experimentally accessible in which $B(p,T) > 0$. Figure 7 shows the variation of the maximum counterflow velocity with temperature (the pressure is the saturated

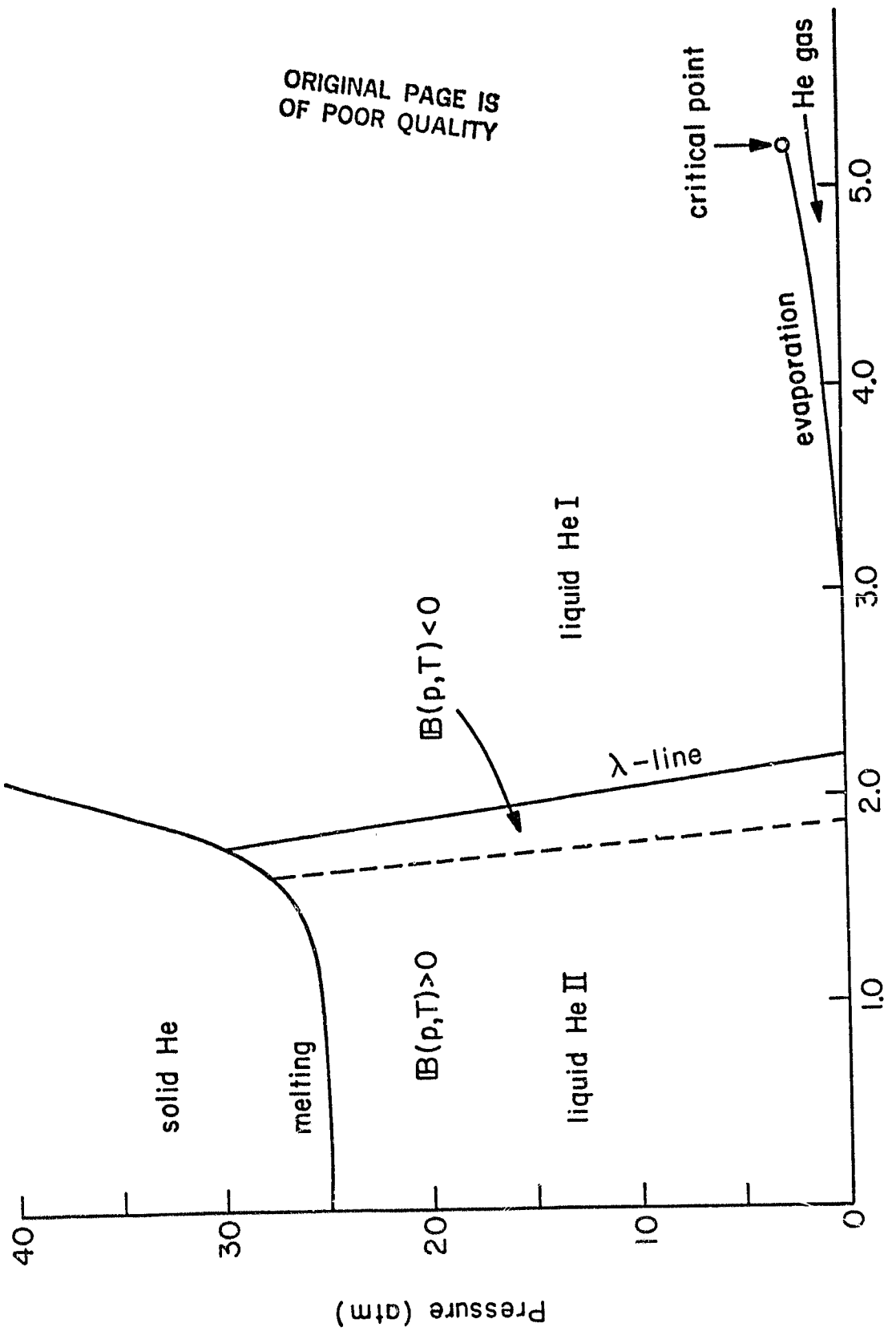

Figure 4. THE FOUR STATES OF ^{4}He IN THE PT PLANE

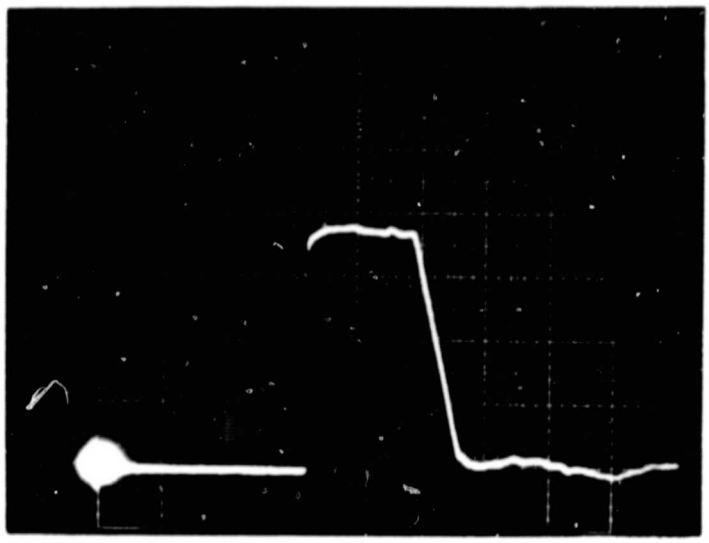

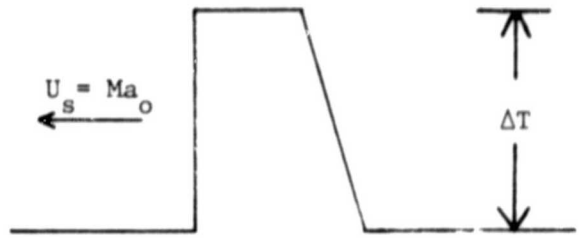

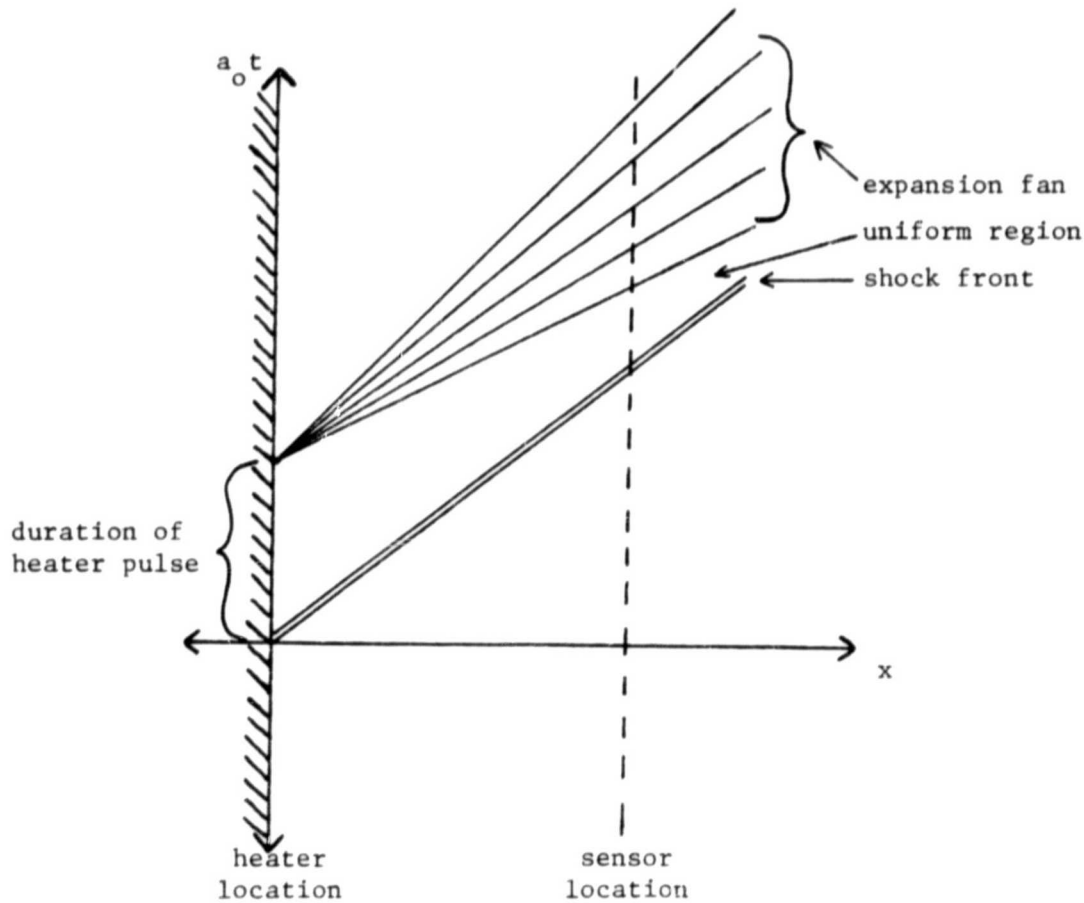

Figure 5. An initially rectangular heat pulse evolves into a shock front, a region of uniform counterflow, and an expansion fan.

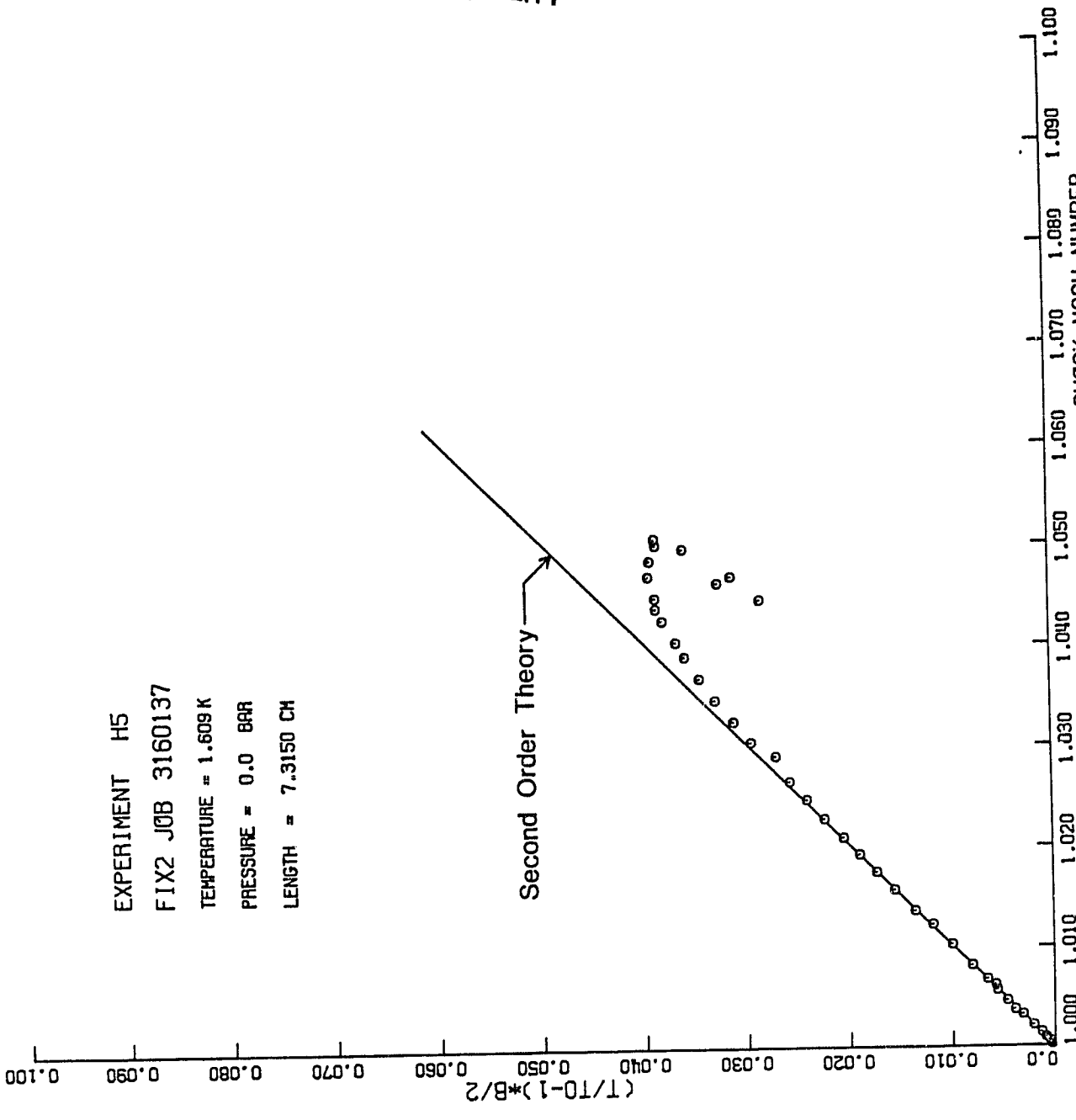

Figure 6. A typical critical velocity experiment.

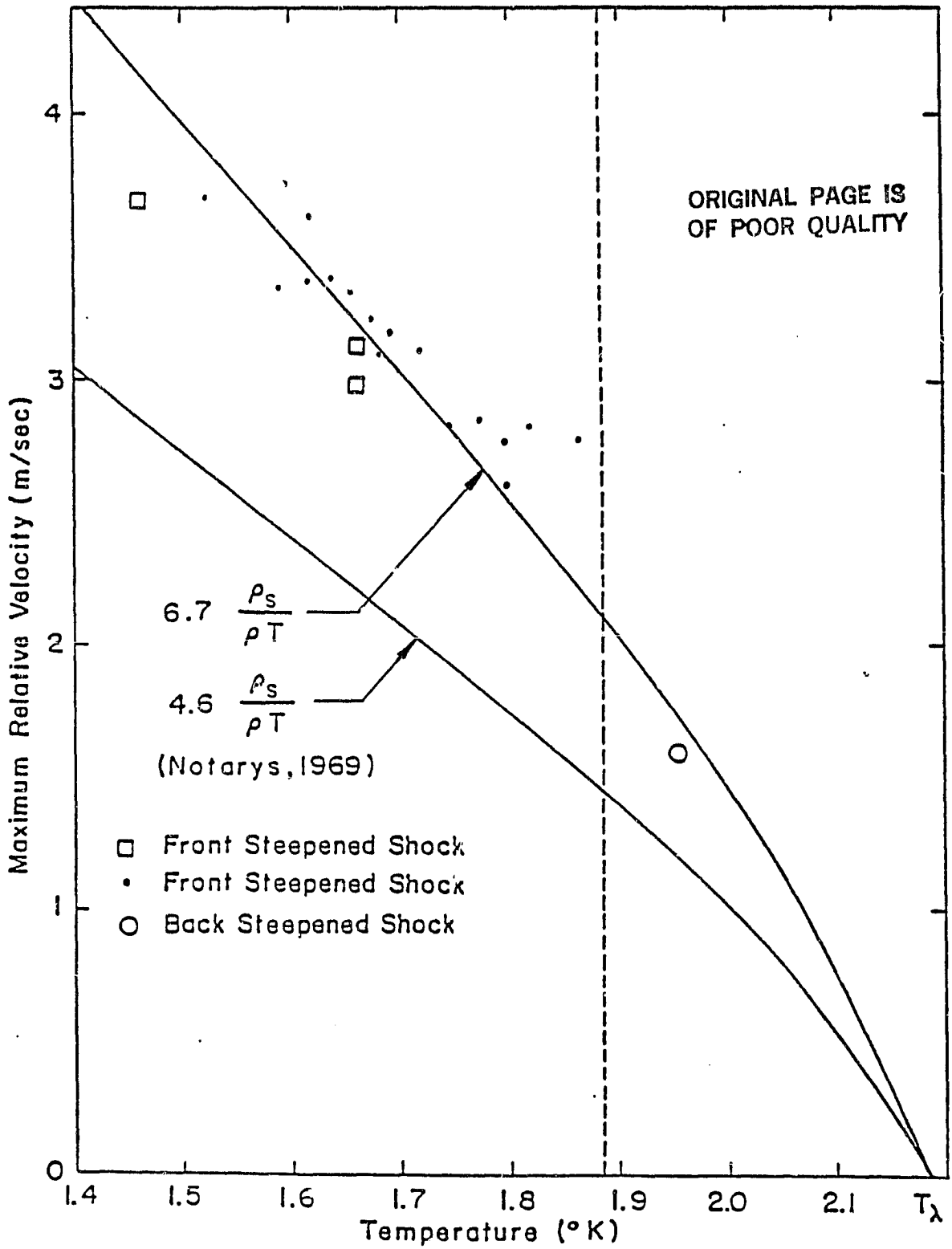

Figure 7. MAXIMUM SHOCK-INDUCED RELATIVE VELOCITY

vapor pressure) and compares the data with the Langer-Fischer prediction for the fundamental critial velocity[6]. The functional dependence on temperature is correct, but the numerical constant is about an order of magnitude lower than the theoretical value.

Another important result coming from such experiments involves the temperature profile of the shock pulse. For relatively low heater powers (the regime in which the second order theory retains validity), a rectangular heat pulse evolves in the typical nonlinear fashion into a shock, a region of uniform counterflow, and an expansion (for $B > 0$), as shown in Figure 5. However, as the heater power is increased, the profile is modified as shown in Figure 8. This modification does not take place gradually as the shock pulse travels down the shock tube; rather, it occurs in the vicinity of the heater. The only amplitude decay of the pulse during propagation, right at the shock front, does not result directly from breakdown but merely comes from the shock/expansion coincidence. This was revealed by using the variable length shock tube to observe repetitions of the same shock strength at different distances from the heater. Therefore, outside of the breakdown region, the points of the temperature profile travel at their characteristic velocities without decaying (except for the shock front as discussed).

This development led to one of the ongoing research efforts. In some sense, if the critical velocity is being exceeded right at the heater, it still is not being observed "out in the bulk fluid, away from walls". To observe larger relative velocities in the bulk fluid, it is necessary to strengthen the shock wave away from the heater. One way to do this is to produce a spherically converging second sound shock wave. It can be shown quite generally for weak waves[8] in a converging channel that

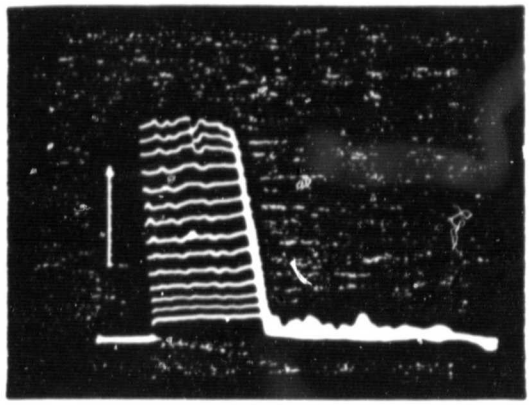

(a) Simple Formation

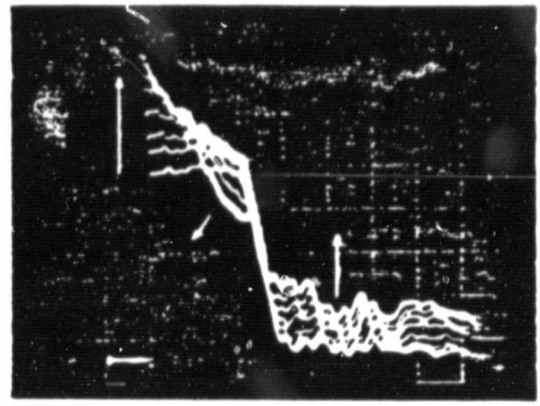

(b) Wave Modification

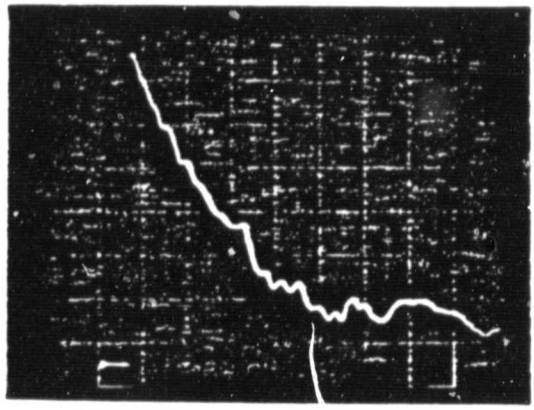

(c) Shock Limit

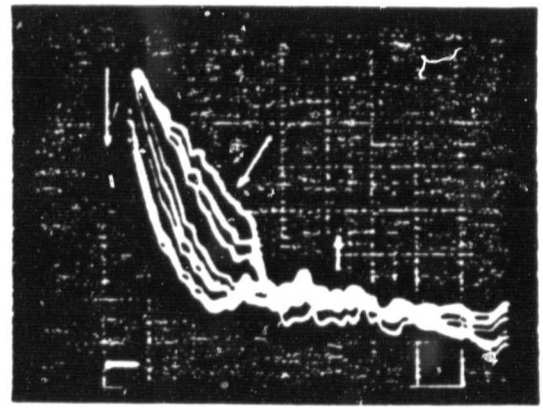

(d) Beyond the Shock Limit

Figure 8 EFFECTS OF HEATER POWER ON SHOCK PULSE PROFILES (200 μsec/division)

$$\frac{M(x)-1}{M(x_0)-1}=\left[\frac{A(x_0)}{A(x)}\right]^{\frac{1}{2}}$$

where $M(x)$ is the Mach number of the shock at position x and $A(x)$ is the area of the channel. Therefore, if a spherical shock of radius of curvature r_0 is produced in a conical channel (see Fig. 9),

$$\frac{M(x)-1}{M_0-1}=\frac{r_0}{r_0-x}$$

and as x increases, M increases. Note that this is only valid for $M(x)-1 \ll 1$. Experiments involving measurements of arrival times and temperature jumps will show whether the fundamental critical velocity is exceeded in the bulk fluid.

Back-Steepening and Double Shocks

Observation of the evolution of rectangular temperature pulses has provided another verification of the second order theory of second sound. For a weak pressure shock in a fluid, the Mach number M and the wave strength $\frac{\Delta p}{p}$ are related by

$$M = 1 + \frac{1}{2}\mathrm{D}(p_0,T_0)\,\frac{\Delta p}{p}$$

$$\mathrm{D}(p,T) = p\left[\frac{\partial}{\partial p}\right]_S \ln(\rho c)$$

For normal substances $\mathrm{D} > 0$ and a positive pressure pulse steepens at the leading edge. For unusual substances (or near the thermodynamic critical point),

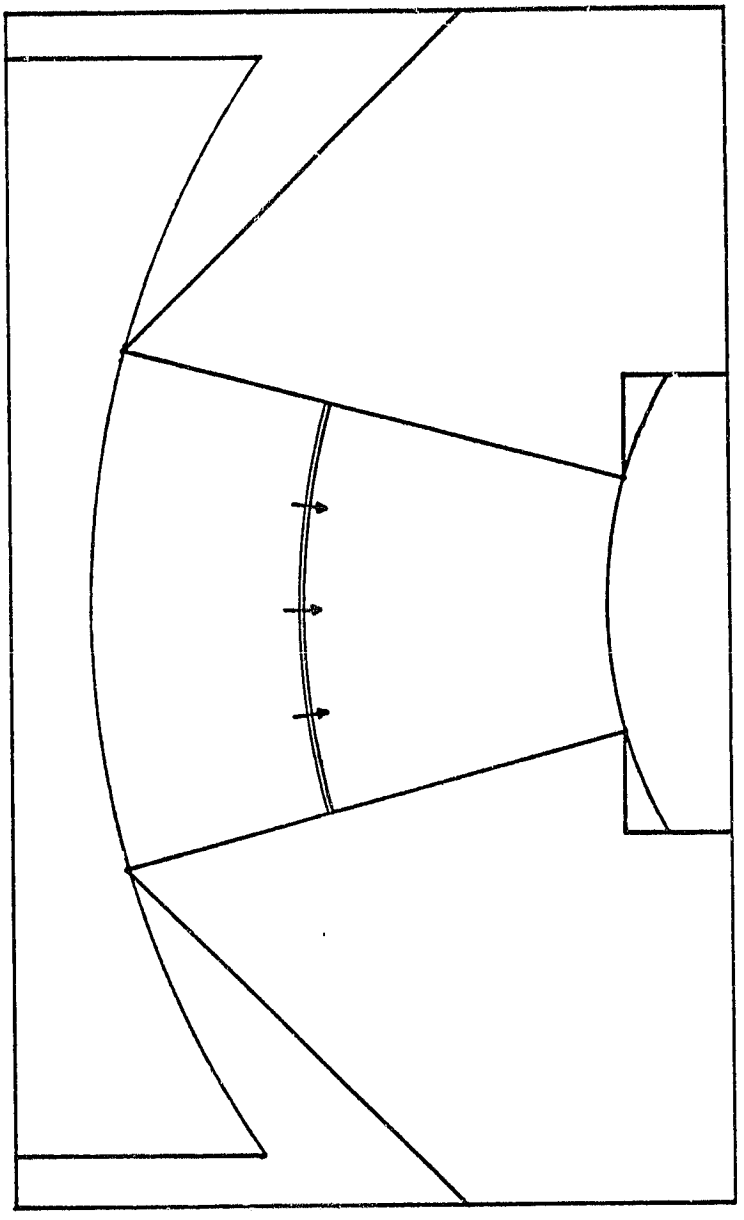

Converging Channel Shock Tube

$$\frac{M - 1}{M_o - 1} = \sqrt{\frac{A_o}{A}} = \frac{r_o}{r}$$

Figure 9. A spherical converging second sound shock strengthens as it propagates.

it is possible to have $D < 0$. In these regions, a positive pressure pulse will steepen at the rear. For weak temperature shocks in superfluid helium, the Mach number and shock strength are related by

$$M = 1 + \frac{1}{2}B(p_o,T_o)\frac{\Delta T}{T}$$

$$B(p,T) = T\left(\frac{\partial}{\partial T}\right)_p \ln\left(\frac{a^3 c_p}{T}\right)$$

Along the saturated vapor curve, $B(p,T)$ is positive from 0.95 K to 1.88 K and negative from 1.88 K to 2.18 K. In the region that $B < 0$, a positive temperature pulse will steepen at the rear. If T_o is slightly less than 1.88 K, where $B(p_o,T_o)$ is slightly positive, the nonlinear relation shows that finite amplitude waves will steepen at both the front and rear, forming a double shock configuration (see Fig. 10). This has been verified experimentally, again demonstrating the validity of the second order theory.

Successive Shock and Rotating Experiments

All of the above experiments have not given much insight into just what happens when the fundamental critical velocity is exceeded. Therefore, it is desirable to examine the flows behind the shocks in order to learn more about this dissipative interaction. It is believed that, when the fundamental critical velocity is exceeded, vorticity (particularly quantized line and ring vortices in the super component) is produced in the flow field behind the shock. These vortices provide the means for momentum transfer between the normal and super components, so in their presence the relative velocity will decay. To examine this idea, it is useful to probe the flow remaining after the passage of a second sound

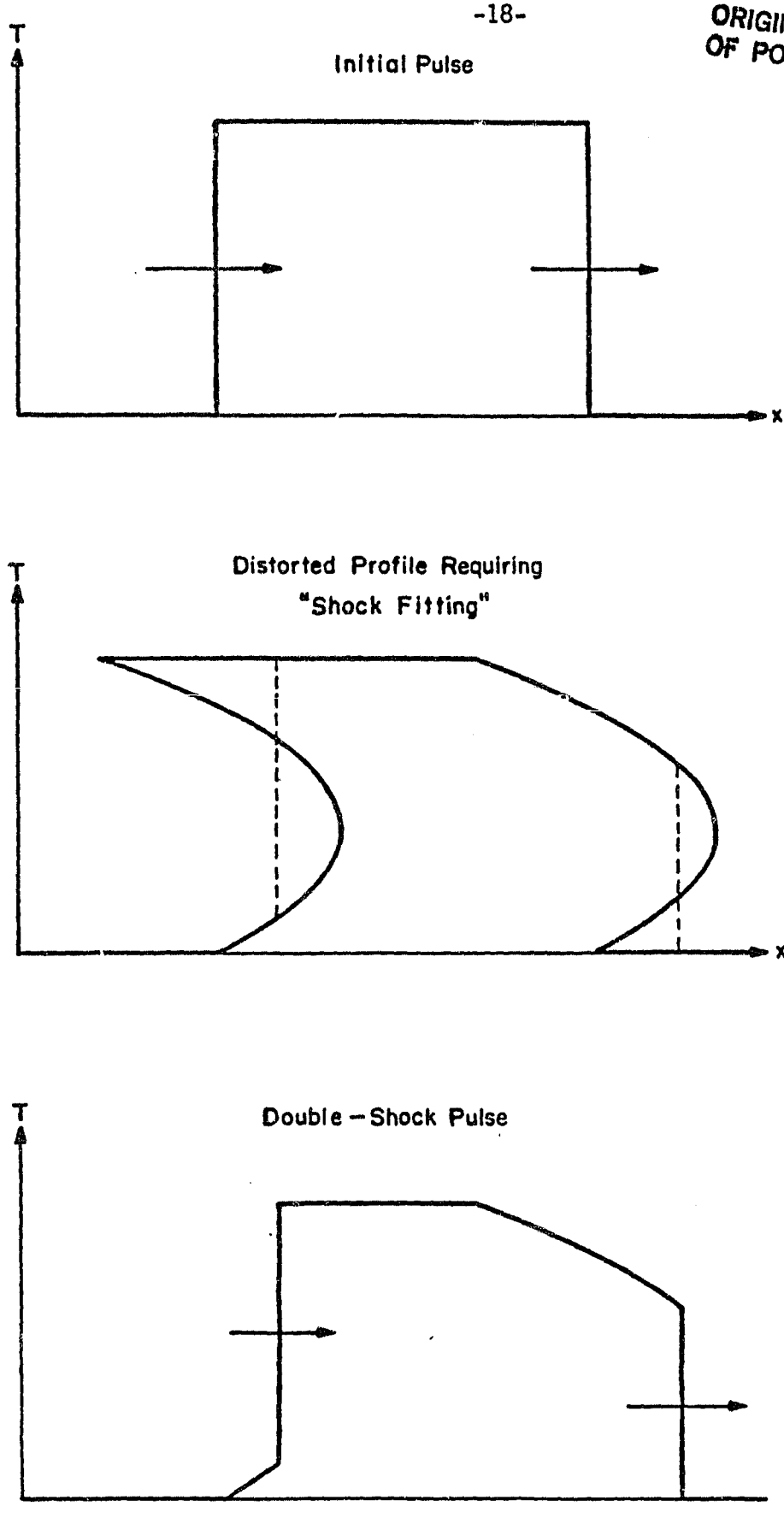

Figure 10. The evolution of a rectangular heat pulse into a double shock profile.

shock with another second sound shock (successive shocks). The results may be compared with experiments involving a shock incident upon a known vorticity field (rotating shock tube).

A typical successive shock experiment would proceed in the following manner. Two second sound shock pulses of identical strength and duration are fired successively, the first into quiescent fluid and the second into fluid processed by the first shock. The time interval between the firings is varied and the resultant waveforms are compared. In all cases, the separation time t_s is far greater than the time it takes for reflections of the first shock pulse to decay completely, so this is not a question of observing the interaction between the two shocks but rather the interaction between the second shock and any undecayed disturbances in the fluid produced by the passage of the first shock.

It turns out that effects of varying the separation time t_s are most dramatically displayed for shocks near the breakpoint (the strength $\frac{\Delta T}{T}$ at which arrival time data begins to deviate from the second order theory). If t_s is large, on the order of several minutes, the waveforms of the two shock pulses are identical (the typical trapezoidal pulse profile). As t_s is reduced to a minute, the second profile begins to exhibit the tilted top and warm tail characteristic of a pulse that has undergone breakdown. With the further reduction of t_s to 1 second, the second shock displays a profile typical of a strongly modified pulse, the front followed by a smooth, exponential-like tail (see Fig. 11). Apparently the first shock produced some sort of slowly decaying disturbances in the fluid, which enhanced the dissipation in the second shock.

To examine the idea that the first shock produced vorticity in the flow, experiments with a rotating second sound shock tube were performed. The specific objective of these experiments was to see how the presence of vorticity would

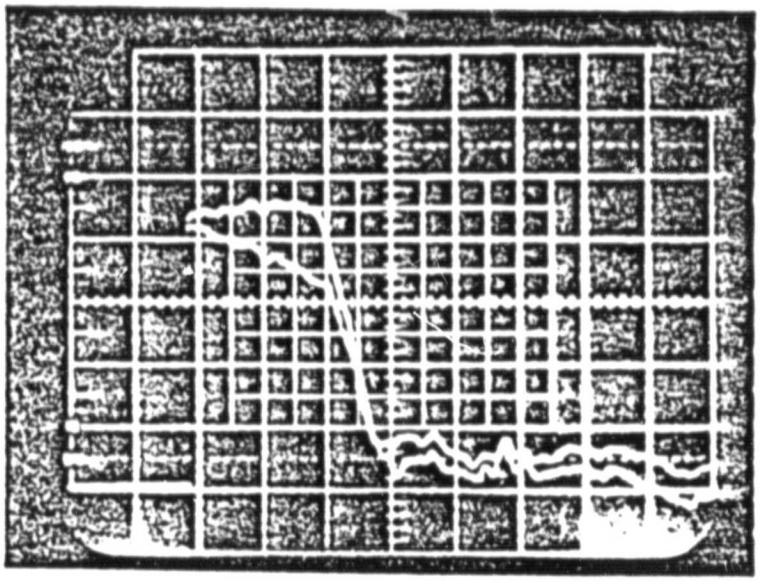

200 μ sec / division

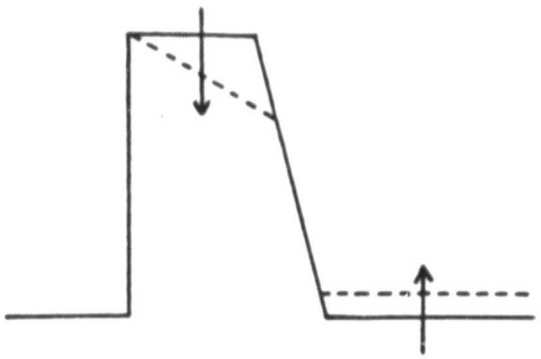

Figure 11. Arrows in direction of decreasing time interval between successive shocks.

—— Several minutes between successive shocks.

--- 1.0 second between successive shocks.

affect a second sound shock pulse. If the profile of a second sound shock pulse were modified by vorticity in the same way that it is by the "fluid disturbances" produced by the first shock in the successive shock experiments, then this is strong evidence that vorticity is produced during breakdown.

Experiments performed in which the shock propagation direction was normal to the axis of rotation (transverse mode) have shown that as the rotation rate Ω is increased, the waveform changes in a manner qualitatively similar to that of the second shock when decreasing the separation time t_s. One difference is that in the rotating case the top of the trapezoidal pulse becomes convex (see Fig. 12) rather than tipping abruptly. This may be a consequence of the uniformity of the vorticity in the rotating case ($\vec{\omega} = 2\Omega\ \hat{e}_z$), whereas in the successive shock case $\vec{\omega}$ is probably randomly oriented; however, the explanation is unclear at the moment.

Future experiments in this area will accomplish several goals. First, the variable length shock tube will be used to characterize the decay of the second shock in the successive shock experiment in terms of the initial shock strength, the separation time, and the region in which decay occurs (at the heater or all along the tube). Next, the variable length shock tube will be used in the rotating dewar to examine the effects of vorticity along the direction of shock propagation, answering questions of whether decay occurs, whether it occurs at the heater or throughout the shock tube, and how the decay depends on the rotation rate Ω. Also, the rotating shock tube will be used to continue studying the decay of shock pulses travelling normal to the rotation axis.

Schlieren Experiments

Another recent research effort has involved using optical techniques to study second sound shock waves in superfluid helium. As is typical of liquids, helium

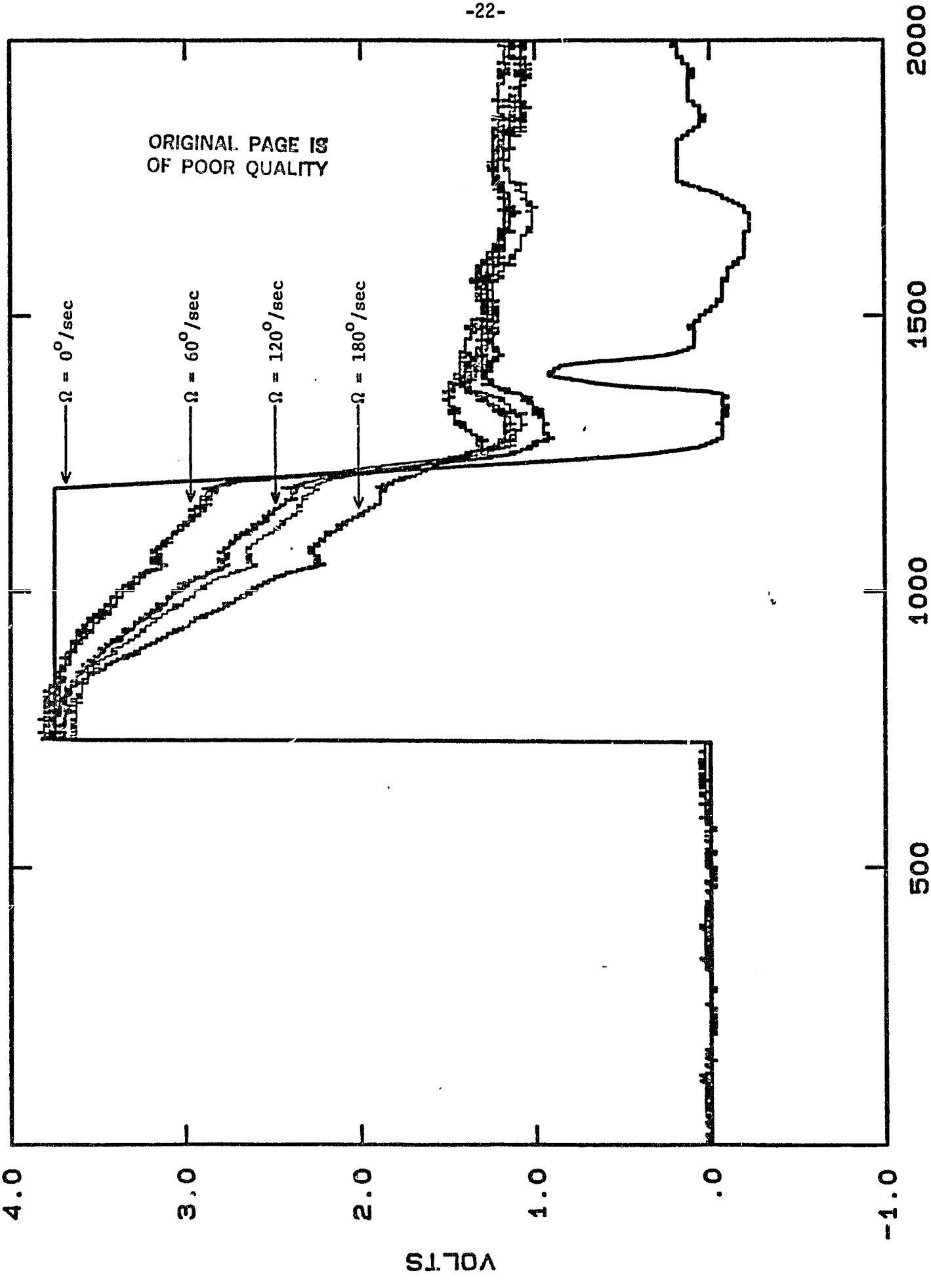

Figure 12. Increasing rotation rate enhances dissipation in a second sound pulse (transverse mode).

has an index of refraction n that is a function of temperature and pressure, so that a change in thermodynamic state produces a change in index of refraction. One of the best techniques to observe variations in n is the schlieren technique (see Fig. 13). Schlieren involves the measurement of the gradient of n along one direction in a test section. Light from a monochromatic slit source is made parallel by the first lens before entering the test section. While traversing the test section, the beam is deflected by the variations of n within the fluid. After passing through the test section, the beam is focused by a second lens. A knife edge (in our case, a razor blade) at the focus intercepts part of the light, while the rest is focused by the third lens on the image plane of a camera or screen. The system is sensitive to the gradient of n perpendicular to the knife edge (in the plane normal to the optical axis).

Experiments to date have used a schlieren system, like that shown in Figure 13, together with an optical dewar and the optical second sound shock tube to visualize second sound shock waves. Figure 14 shows one such picture. The bright line is the leading (temperature raising) second sound shock in a double shock pulse (see above for an explanation of double shocks), and the dark line is the trailing (temperature lowering) shock. The two shocks produce opposite effects in the schlieren system because their gradients of n are oppositely directed. Other photographs at later times show that the fronts remain planar even after multiple reflections from the endwalls. Figure 14 shows two image-processed pictures of a strong shock which has undergone breakdown (the shock is travelling downward in these two pictures). The first picture shows the shock front followed by the exponential-like tail (a bright line followed by a dark region). Printed on this picture also is the gray level distribution, which allows generation of contrast-enhanced pictures as in Figure 14. Pictures such as these may aid in studying the flows produced behind the shock front. The schlieren system has also been used to study second sound shocks obliquely

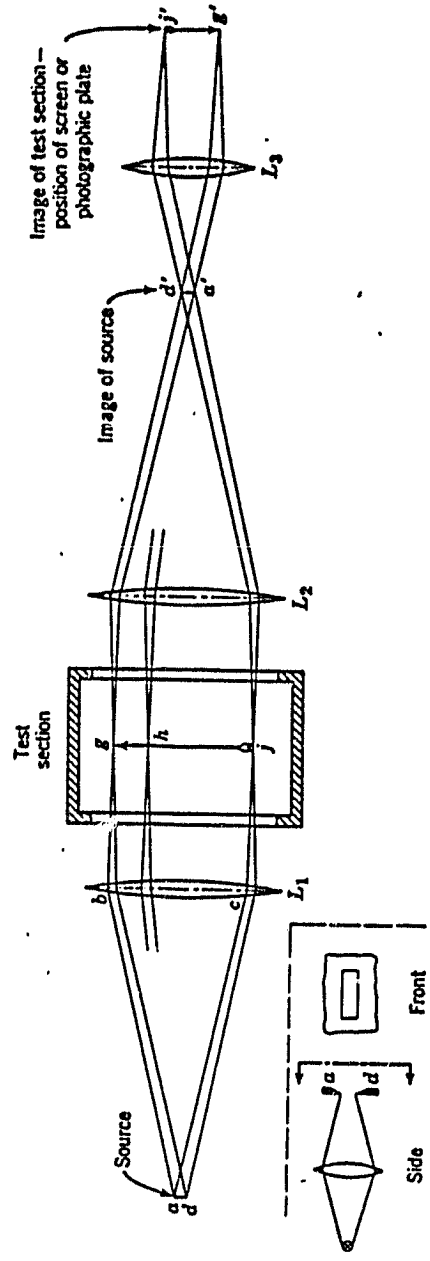

FIG. 13 Schlieren system with lenses. Inset: detail of system for forming rectangular source.

Figure 14. Schlieren photography of second sound shocks.

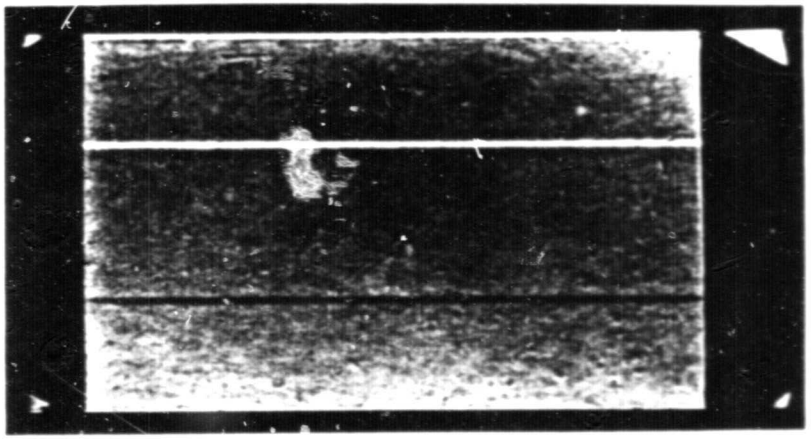

Double shock pulse.

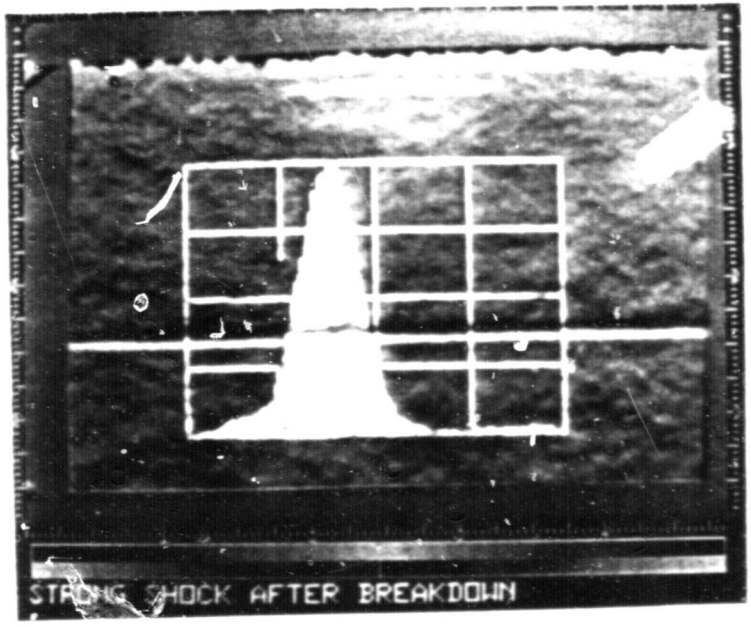

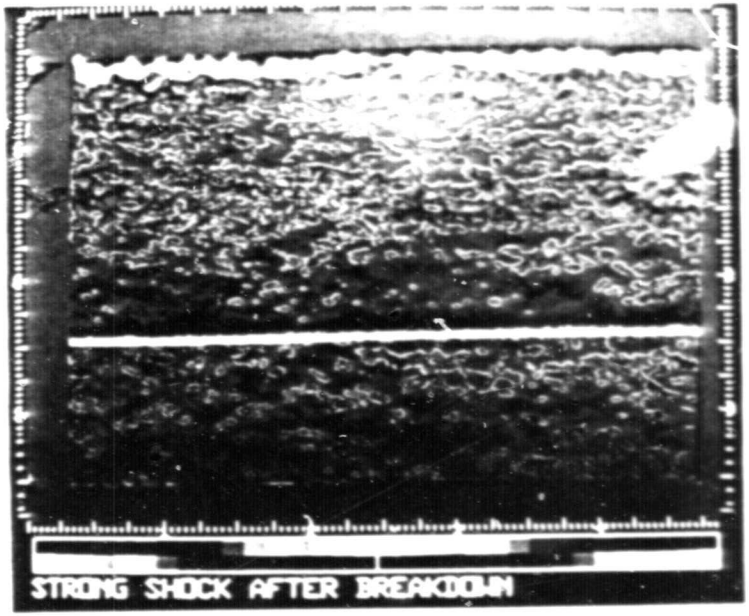

Image-processed photographs of a strong shock (color enhanced).

incident on a liquid-vapor interface.

Scattering Experiments

It is possible to use scattering of high frequency second sound to image flow fields in helium just as it is possible to use first sound to image flow fields in ordinary fluids[9]. Preliminary experiments have observed scattering from thin wires placed in liquid helium. It is hoped that scattering of second sound will allow imaging of arrays of quantized vortices as well as real time observation of vortex dynamics.

Conclusion

Use of second sound techniques to study superfluid helium has proved to be extremely fruitful. Second sound shock waves have produced relative velocities in the bulk fluid orders of magnitude larger than previously observed. Maximum counterflow velocites produced in this way are found to follow the Langer-Fischer prediction for the fundamental critical velocity in its functional dependence on temperature and pressure. Comparison of successive shock and rotating experiments provides strong evidence that breakdown results in vorticity production in the flow behind the shock. Schlieren pictures have verified the planar nature of second sound shocks even after multiple reflections. The nonlinear theory of second sound has been repeatedly verified in its prediction of double shocks and other nonlinear phenomena.

1. References

1. T. N. Turner, Ph.D. Thesis, California Institute of Technology (1979).

2. J. R. Clow and J. D. Reppy, Phys. Rev. Lett. **19**, 291 (1967).

3. H. A. Notarys, Phys. Rev. Lett. **22**, 1240 (1969).

4. G. B. Hess, Phys. Rev. Lett. **27**, 977 (1971)

5. D. H. Liebenberg, Phys Rev. Lett. **26**, 744 (1971)

6. J. S. Langer and M. E. Fischer, Phys. Rev. Lett. **19**, 560 (1967).

7. I. M. Khalatnikov, *Introduction to the Theory of Superfluidity*, Benjamin, New York (1965) (see Chapter 13).

8. G. B. Whitham, *Linear and Nonlinear Waves*, John Wiley & Sons, New York (1974).

9. B. O. Trebitz, Ph.D. Thesis, California Institute of Technology (1982).